Dielectric behaviour versus temperature of a monoepoxide

1997 J. Phys.: Condens. Matter 9 6199

(http://iopscience.iop.org/0953-8984/9/29/006)

J. Phys.: Condens. Matter **9** (1997) 6199–6216. Printed in the UK PII: S0953-8984(97)82487-3

Dielectric behaviour versus temperature of a monoepoxide

S Corezzi†, S Capaccioli†, G Gallone‡, A Livi† and P A Rolla†

† Institute for Physics of Matter (INFM) and Department of Physics, University of Pisa, Piazza Torricelli 2, 56126 Pisa, Italy

‡ Institute for Physics of Matter (INFM) and Department of Chemical Engineering, University of Pisa, Italy

Received 11 March 1997, in final form 6 May 1997

Abstract. The conductivity and dielectric relaxation behaviour of a glass-forming monoepoxide, cresyl glycidyl ether (CGE), were studied from 10^2 to 10^7 Hz by impedance spectroscopy, in the temperature interval 83–333 K. Data analysis indicated the existence of a transition temperature $T_B \cong 265$ K marking the separation between two different relaxation regimes, in accordance with previous results given by Stickel and co-workers. The temperature T_B is well above the glass transition temperature ($T_g = 204$ K), and coincides with the temperature at which the timescales of the main and secondary relaxation processes coincide, so at $T > T_B$ there is a unique overall relaxation process. The splitting layout of CGE differs from that of the very common diepoxide diglycidyl ether of bisphenol-A (DGEBA), studied previously, and also the relaxation at high temperature has a correspondingly different dynamical behaviour. The relaxation strength behaviour is also analysed and compared with that of DGEBA; the similarities are discussed.

1. Introduction

The maxima observed in the relaxational loss spectrum of a complex liquid system change shape and position as the temperature is varied; below a certain temperature, where the system apparently becomes an amorphous solid, some of them disappear [4]. It is said that the system has been undercooled in a glassy state. The glass transition determines the mechanical properties of a number of materials which are extremely important in modern structural applications, so this phenomenon has been widely studied for many years, although a fully satisfactory explanation has not yet been achieved [5, 6]. One of the main aspects of the discussion of the glass transition concerns the microscopic origin of the relaxation processes which are observed when the system is driven by an external time-varying force. The system relaxes by internally dissipating a certain amount of the energy transferred to it; this behaviour produces a response delayed in time with respect to the external force, and it can be described in the frequency domain by a complex transfer function. The internal dissipation occurs through microscopic motions of various natures, which are determined either by the specificity of the molecular structure or by local molecular arrangements. Generally, the two cases can be simultaneously verified. At the glass transition, packing of the molecules and blocking of their long-range diffusive motions occur; the residual active relaxations, i.e. the secondary relaxations, can be related either to localized diffusive processes allowed by the molecular packing [7–11] or to intramolecular motions of specific segmental or side molecular groups [12–17]. However, in our opinion, such effects cannot be entirely distinguished, and the experimental results do not lead to unambiguous conclusions.

0953-8984/97/296199+18$19.50

Significant information can be extracted from comparing experimental data obtained by different techniques, such as dielectric spectroscopy, light and neutron scattering, dynamical thermal and mechanical analysis, and magnetic resonance spectroscopy [18–24]; however, as different observables are involved, a quantitative comparison might be not sufficiently accurate.

As regards the investigation the relaxation phenomena in complex fluids, dielectric spectroscopy is characterized by great sensitivity over an unsurpassed wide frequency range, and can provide significant results. In particular, two different observables can be simultaneously measured: the conductivity and the complex dielectric permittivity. These two observables can be, to some extent, quantitatively related to enhance the information on the dynamics of the system. The extraction of information from dielectric data needs a suitable model, i.e. a relaxation function, whose parameters can be accurately determined through a fitting procedure, provided that the experimental data are numerous and sufficiently accurate. The accuracy of modern dielectric wide-band experimental techniques, ranging from mHz to some tenths of GHz, has improved the analysis of the conductivity and relaxation time data versus temperature [1, 2], and permits one to reliably extract additional information, i.e. the relaxation strength and shape, and to study in more detail the coupling of different relaxation modes [18, 25, 26].

In this paper, we discuss the analysis of the dielectric relaxation behaviour versus temperature of a glass-forming system, cresyl glycidyl ether (CGE). This system was chosen for its similarity with diglycidyl ether of bisphenol-A (DGEBA), studied previously [25]. In both systems the main dipole moment is located on the ether group, but DGEBA carries two ether dipolar groups at its ends, while CGE has only one.

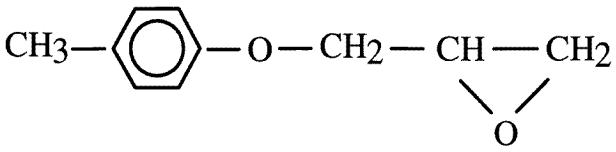

Figure 1. The molecular structure of CGE.

2. Experimental procedure

The system tested was a commercial-grade (manufactured by Shell) monoepoxide, 1, 2-epoxy-3-tolyloxy-propane, also known as cresyl glycidyl ether (CGE), whose molecular weight is 164.22. The molecular structure is displayed in figure 1.

The dielectric measurements were carried out using an HP4194A impedance analyser. The instrument was connected via an IEEE488 standard interface to a personal computer; the software was specifically developed to execute the measurement procedure, and to store and pre-analyse the collected data. Measurements were carried out at temperatures from 83 K to 333 K. First, the sample was very quickly cooled down to the lowest temperature, and then slowly heated by a dry nitrogen flow whose temperature was stabilized by an electronic proportional controller; measurements were made after thermal equilibrium was reached. The thermal stability was ± 0.1 K. The spectra of the dielectric permittivity were calculated from the complex admittance data for a cylindrical capacitor cell filled with the sample. The admittance was calculated by averaging 64 readings carried out for 200 different frequency values within the range $10^2 - 10^7$ Hz. The empty-cell capacitance ($\cong 2.4$ pF) was determined at the beginning of the experiment by filling the cell with cyclohexane.

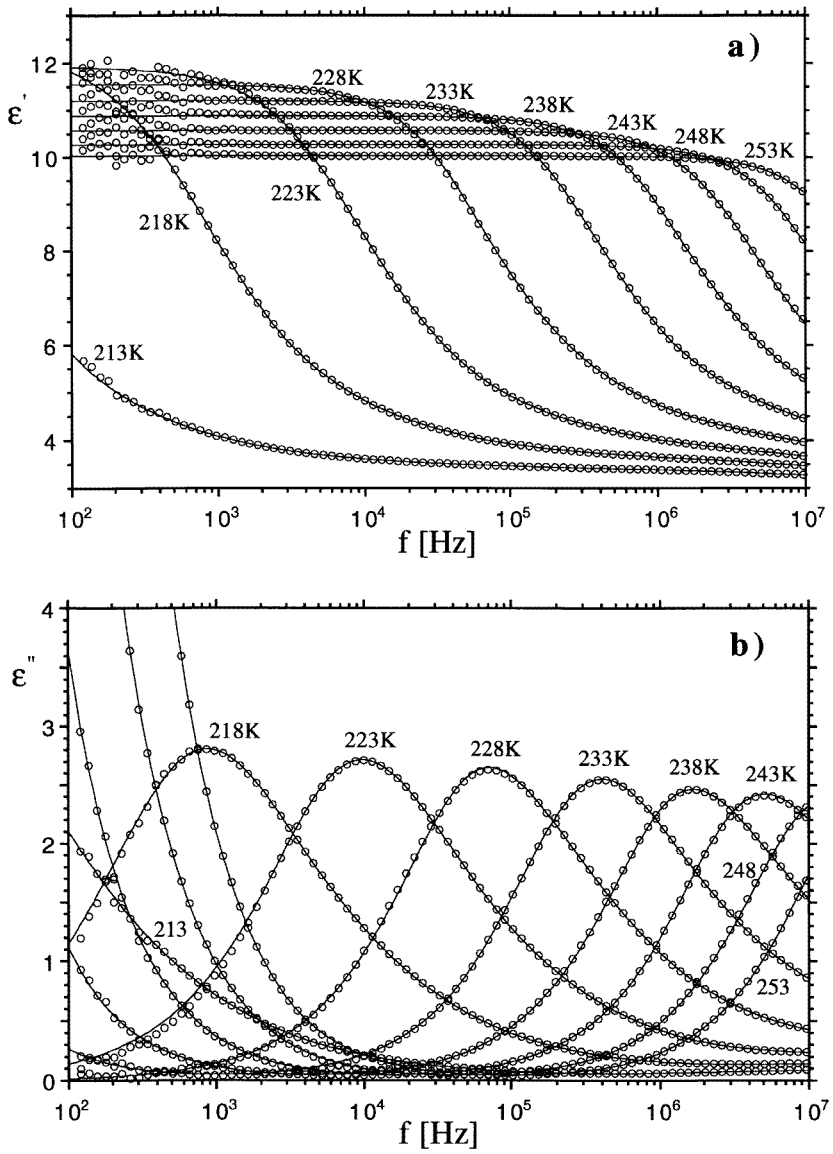

Figure 2. Dielectric spectra: (a) ε' and (b) ε'' versus frequency at different temperatures (degrees Kelvin) above the glass transition temperature. The solid lines represent the fitting equation (1)—see later.

3. Results and discussion

The dielectric spectra of CGE for different temperatures are shown in figure 2(a) and 2(b); the maximum of the dielectric loss factor, ε'', spans four decades of frequency when temperature is varied between 218 K and 243 K. At the highest temperatures, a conductivity contribution is recognized in the low-frequency end of the ε''-spectrum; in fact, ε'' rises as the frequency decreases, while ε' remains stable. The solid lines in the figures represent the fitting equation (1), as will be discussed later.

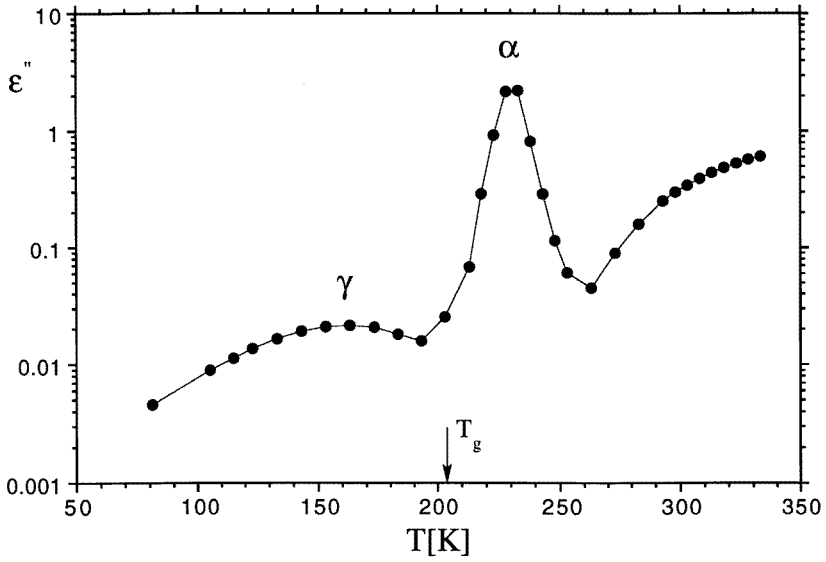

Figure 3. ε'' as a function of temperature at 200 kHz. The solid line is a guide for the eye only.

The spectra at 218 K and 223 K in figure 2(a) show that ε'-values at high frequencies are higher than would be expected for a completely unrelaxed polarization, while the corresponding values of ε'' in figure 2(b) do not decrease as they should; this suggests the presence of a relaxation process at higher frequencies. To obtain a complete picture of the relaxation processes, ε'' was measured at the fixed frequency of 200 kHz by varying the temperature. The corresponding plot, reported in figure 3, shows the existence of two relaxations: the most intense (α) is the same as that observed in figures 2, while the smaller one (γ), very broad indeed, looks like a secondary relaxation occurring below the glass transition temperature T_g of the system. The spectra obtained by progressively heating the system from 153 K to 213 K describe this small and broad relaxation process better (figures 4(a) and 4(b)). The frequency window, however, is not wide enough for us to observe simultaneously the maxima of both—the main and secondary—relaxations; the secondary one appears in the frequency window at about 210 K in the tail of the main relaxation (see the spectra at 213 K and 203 K in figure 4(b)). From the spectra of figures 2(a), 2(b), 4(a), and 4(b), Cole–Cole plots for different temperatures were obtained (shown as figures 5(a) and 5(b)). Figure 5(a) shows the Cole–Cole plots of the main relaxation at different temperatures. At the low-frequency end, the conductivity contribution (data going upward) disappears as the temperature decreases, while the small contribution of the secondary relaxation appears at the high-frequency end as the temperature decreases. The secondary relaxation is plotted in figure 5(b) for temperatures below the glass transition temperature. The solid lines in figures 5(a) and 5(b) represent the fitting equation (1) (see below) plus the conductivity term.

The presence of two relaxations was also revealed for a low-molecular-weight commercial-grade DGEBA resin (EPON828 manufactured by Shell) [25, 27]. Pochan *et al* [12] analysed commercial-grade DGEBA resins of different molecular weights, and revealed three relaxation processes: the main one, as usual labelled with the letter α, was related to the orientational motion of the whole molecule; the secondary one, which occurs at intermediate temperatures or frequencies, was labelled as β, and was attributed to a

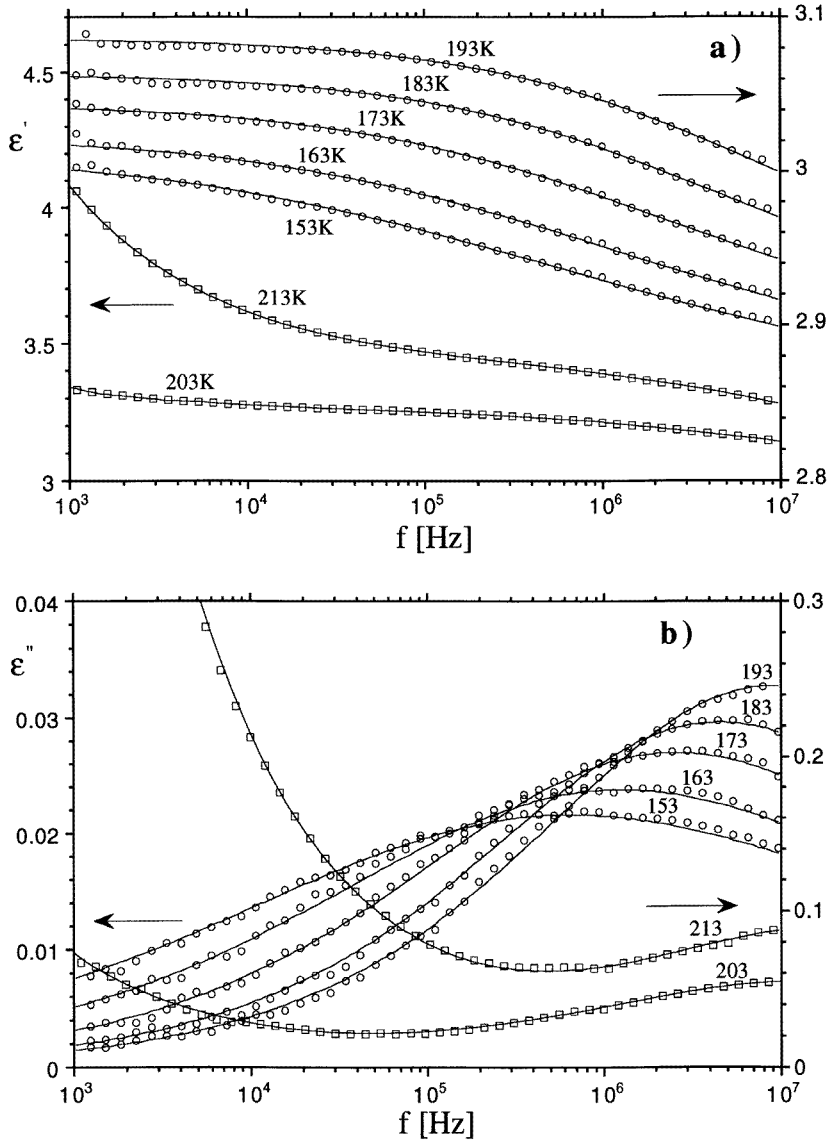

Figure 4. Dielectric spectra: (a) ε' and (b) ε'' versus frequency at different temperatures (degrees Kelvin) through and below the glass transition. The values of ε' at 203 and 213 K (squares) must be read from the left-hand axis; the values of ε'' at the same temperatures (squares) must be read from the right-hand axis. The solid lines represent the fitting equation (1).

segmental motion involving the hydroxyether group. The latter was not observable for the low-molecular-weight resins, since the concentration of hydroxyether groups was negligible. Finally, the other secondary one, found in the low-temperature or high-frequency region, was related to the most mobile dipolar group, i.e. the ether group, and was labelled γ. Accordingly, the two relaxations observed in the low-molecular-weight resin EPON828 were labelled as α and γ, and related to the whole-molecule orientational motions and to the motion of the epoxide groups, respectively. A similar attribution can be proposed for the

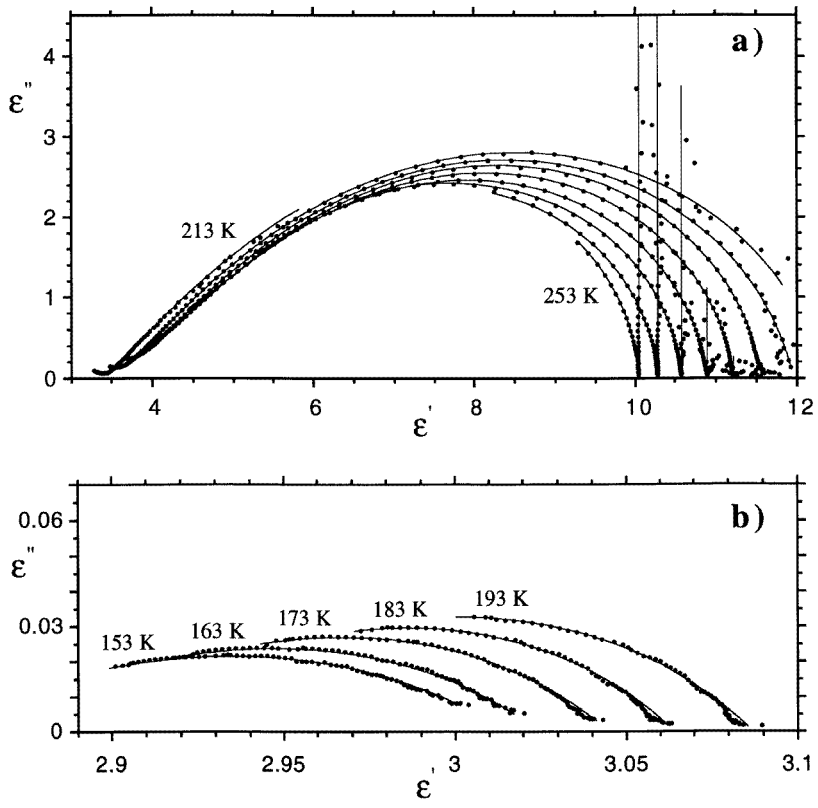

Figure 5. Cole–Cole plots at different temperatures (a) above (the temperatures are the same as in figure 2) and (b) below the glass transition temperature.

present CGE system, and the same labelling, α and γ, is used here. CGE has one epoxide group in each molecule, while DGEBA has two; however, the volume concentrations of the epoxide dipoles in the two compounds are almost the same. Accordingly, the main and secondary relaxation strengths are expected to be almost equal for the two systems. As will be discussed later, this is not verified, and the relaxation strengths of CGE are generally smaller than the corresponding ones of DGEBA. This result can probably be attributed to a different packing of the molecules of CGE with respect to that for DGEBA. In fact, the packing can produce a compensating arrangement of dipoles, as well as some steric hindrances of the molecules which reduce the alignment capability of dipolar groups.

To fit the two relaxation processes, a superposition of two relaxation functions was considered:

$$\varepsilon(\omega) - \varepsilon_2 = (\varepsilon_0 - \varepsilon_1)L_1 + (\varepsilon_1 - \varepsilon_2)L_2 \tag{1}$$

where $L = [1 + (\mathrm{i}\omega\tau)^{1-\alpha}]^{-\beta}$ is the normalized Havriliak–Negami (HN) relaxation function which proved to be suitable for representing the dielectric response of polymers as well as that of low-molar-mass glass-forming liquids [25, 28]; $\varepsilon(\omega)$ is the complex permittivity (ω is the angular frequency); ε_0 and ε_2 are the completely relaxed and unrelaxed dielectric constants, respectively; ε_1 is the relaxed (unrelaxed) dielectric constant of the α-relaxation (γ-relaxation). The real and the imaginary parts of the permittivity were measured for 200 different frequencies, and the two sets of data were simultaneously fitted with the real and

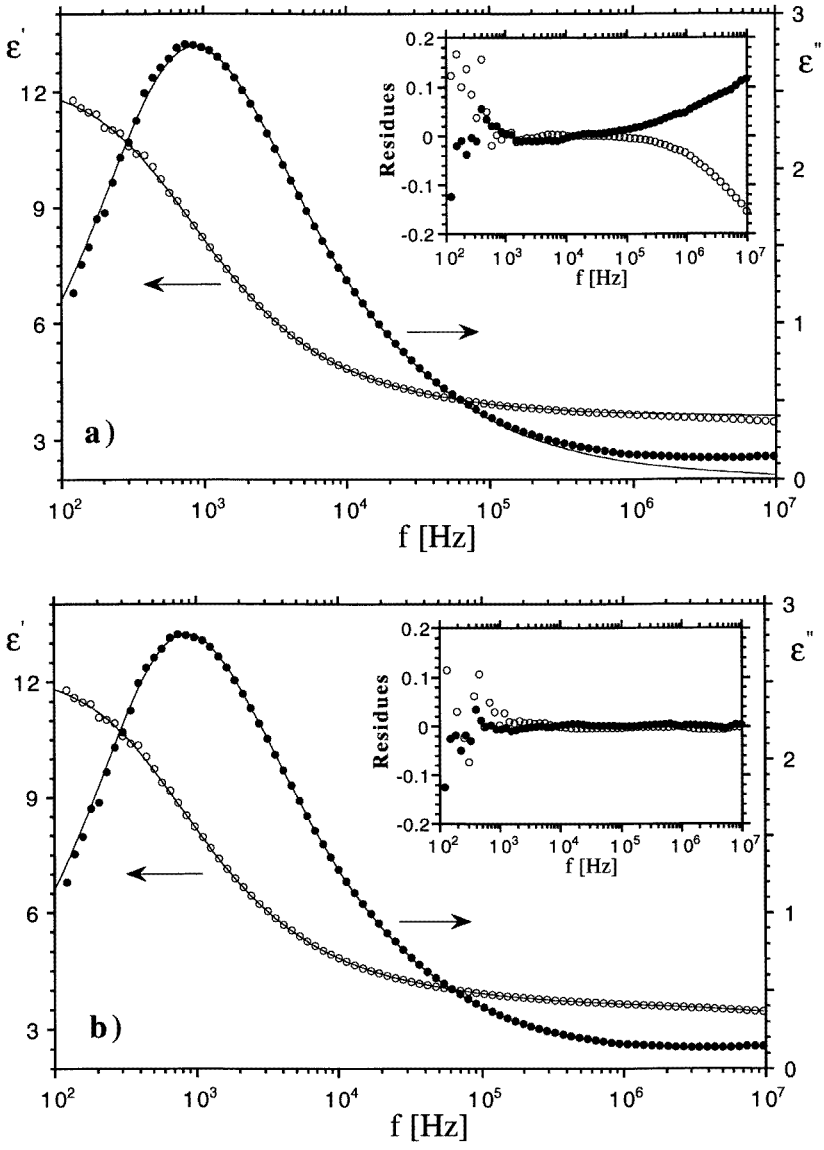

Figure 6. The real (open circles) and imaginary (full circles) parts of the permittivity at 218 K. (a) The solid lines represent the single HN fitting equation ($\varepsilon_0 = 12.35$ and $\varepsilon_2 = 3.6$). (b) The solid lines represent the fitting equation obtained by a superposition of two HN functions ($\varepsilon_0 = 12.35$ and $\varepsilon_2 = 2.9$). The residues originating from the different fitting equations are shown in the insets.

imaginary parts of equation (1), respectively.

A conductivity term, $-4\pi i\sigma/\omega$, was added to the fitting function to account for the drift of charge carriers, generally impurity ions. However, the conductivity parameter, σ, was generally extracted by fitting separately the low-frequency-data of ε'', as the conductivity effect is well separated from the polarization one, particularly for the highest temperatures of the measurement interval (above 243 K up to 333 K).

The differences between a fitting procedure based on a single HN relaxation function and one based on equation (1) are shown in figures 6(a) and 6(b), respectively, for the case where the contributions of the two relaxations are closer to each other, and appear in the experimental frequency window. The high-frequency tails of the spectra cannot be accurately fitted by a single relaxation function, as is demonstrated by the residues in the insets of figure 6(a) and 6(b), which differ appreciably just in the high-frequency part of the spectra. Moreover, the deviation from the experimental data of the fitting curves in figure 6(a) is positive for ε' and negative for ε'': in fact, the second relaxation at higher frequencies lowers the ε'-data and pushes up the ε''-data with respect to the trends relating to the low-frequency single relaxation. In addition, the single-relaxation fit provides a value of $\varepsilon_2 \cong 3.6$, which is larger than that expected for a completely unrelaxed dielectric constant. The fitting curves derived from equation (1) are plotted as solid lines in figures 2(a), 2(b), 4(a), 4(b), 5(a), and 5(b).

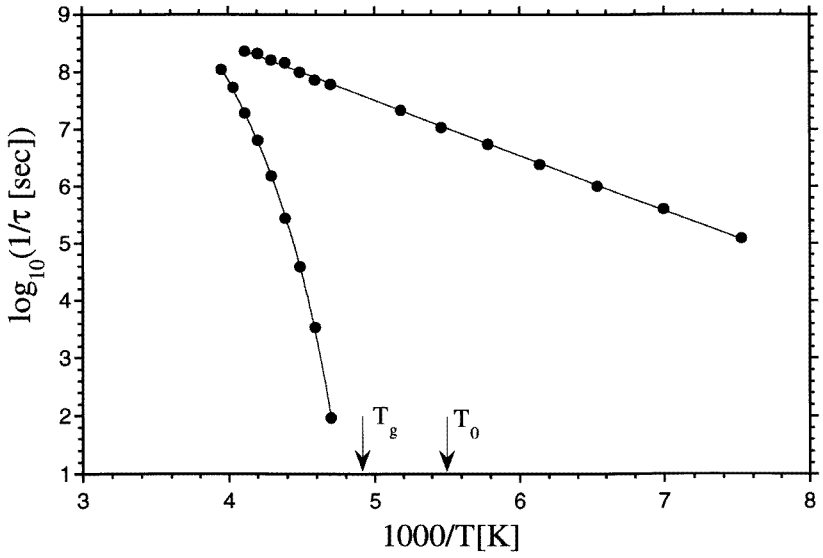

Figure 7. The relaxation times τ of the main and secondary relaxations versus the reciprocal temperature $1/T$. The solid lines represent the fitting equations.

3.1. Relaxation times

The relaxation time parameters were determined in the temperature interval from 133 K to 253 K (those of the main relaxation, from the range 213 K to 253 K; those of the secondary one, from the range 133 K to 243 K) (figure 7). The secondary relaxation times, as usual, show an Arrhenius behaviour, with an activation energy of 4.4 kcal mol^{-1} (i.e. comparable with that of DGEBA: 5.7 kcal mol^{-1}), while the main relaxation time values were conveniently described by the Vogel–Tammann–Fulcher equation (VF) [29, 30]:

$$\tau = \tau_0 \exp[B'/(T - T_0')] \tag{2}$$

where B' is a constant, τ_0 is the relaxation time at very high temperatures, T is the absolute temperature, and T_0' is the temperature at which the relaxation time becomes extremely large. The VF equation was originally proposed to describe the scaling behaviour of the

viscosity η, and extended to describe the dielectric relaxation time, τ, by assuming that τ is proportional to the viscosity, according to the Maxwell model for viscoelasticity.

From equation (2), the following parameter values were determined: $B' = 805$ K and $T_0' = 181$ K.

The glass transition temperature T_g, calculated using the fitting equation for $\tau = 100$ s, was 204 K.

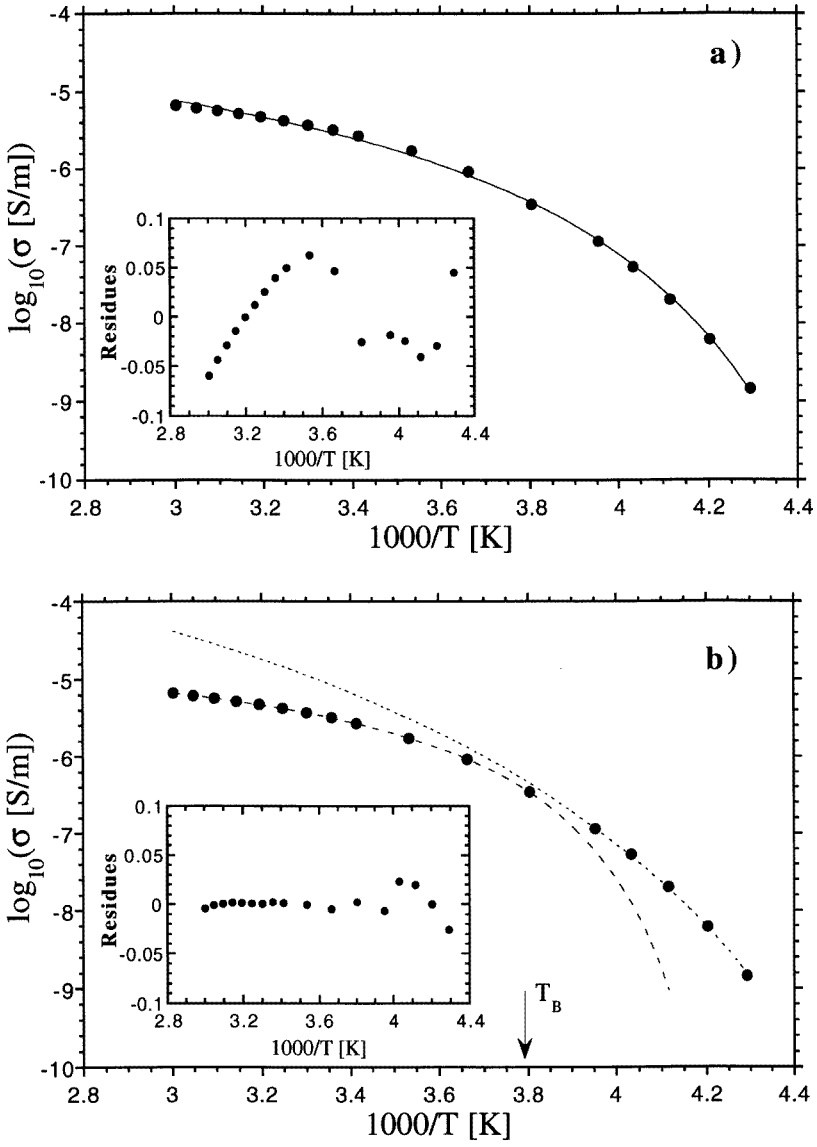

Figure 8. The d.c. conductivity versus the reciprocal temperature $1/T$. (a) The solid line represents the best fit with a single VF equation. (b) Dotted and dashed lines represent the low- and high-temperature VF fitting equations, respectively. $T_B = 265$ K is the temperature at which the transition between the two VF regimes occurs. The insets show the residues.

3.2. Conductivity

The conductivity values, determined in the temperature interval from 233 K to 333 K, have been drawn in figure 8(a). In the temperature interval explored, well above the glass transition temperature ($T_g \cong 204$ K), the conductivity σ, generally originating from impurity ions, is related to the viscosity of the system by the following equation:

$$\sigma\eta = ne^2/6\pi r. \tag{3}$$

Equation (3) is obtained by combining the Einstein relation between the diffusion coefficient D_i of the ions and the d.c. conductivity:

$$D_i = \sigma k_B T/ne^2 \tag{4}$$

where k_B is the Boltzmann constant, n the number of charge carriers per unit volume, and e the electron charge, with the Stokes–Einstein equation:

$$D_s = k_B T/6\pi r\eta \tag{5}$$

which provides the translational diffusion coefficient D_s of a sphere of radius r moving in a continuous medium of viscosity η. Equation (3) is obtained under the condition $D_i \cong D_s$. This result is based on a hydrodynamic model which is generally verified for the motion of ions embedded in a medium of comparable molecular size in order to ensure the required coupling between the ions and the surrounding molecules.

In the absence of any charge-generation mechanism, the quantity on the right-hand side of equation (3) should be stable against temperature variation. In particular, under these conditions, assuming that the viscosity scales according to the VF law, the same scaling behaviour should be verified also for conductivity:

$$\sigma = \sigma_0 \exp[-B''/(T - T_0'')] \tag{6}$$

where B'' is a constant, T_0'' is the temperature at which the conductivity ideally reduces to zero, and σ_0 is the conductivity at very high temperatures.

The experimental data seem to be suitably fitted by equation (6) (figure 8(a)), and the following parameters were obtained: $B'' = 336$ K and $T_0'' = 203$ K, which are markedly different from those obtained for the relaxation times. This result could be reasonable for the B-parameter, the conductivity and relaxation time being related to different microscopic mechanisms; but it is surprising for T_0, which is considered as a limit temperature at which all diffusive motion has stopped. However, it has to be taken into account that the data to which the fit was performed in the two cases pertain to temperature intervals that only partially overlap. By repeating the fit on the five conductivity data at the lowest temperatures (figure 8(b)), we obtained parameters ($B'' = 794$ K; $T_0'' = 182$ K) closer to those of the relaxation times fit for the same temperature interval, while the residual conductivity data were conveniently fitted by a different VF equation ($B'' = 156$ K; $T_0'' = 228$ K).

3.3. Comparison of conductivity and relaxation time data

According to equation (3) and to the Maxwell model, the conductivity and relaxation time are simply related:

$$\sigma\tau = \text{constant}. \tag{7a}$$

Equation (7*a*) has been widely verified for low-molar-mass systems for temperatures well above the glass transition temperature. For more complex systems, including polymers, the

conductivity and relaxation time above T_g were experimentally found to be related by the equation [31, 32]

$$\sigma \tau^s = \text{constant}. \tag{7b}$$

Equation (7*b*) can be derived by free-volume theory, and the exponent s is related to the ratio between ionic and segmental mobility [31, 33].

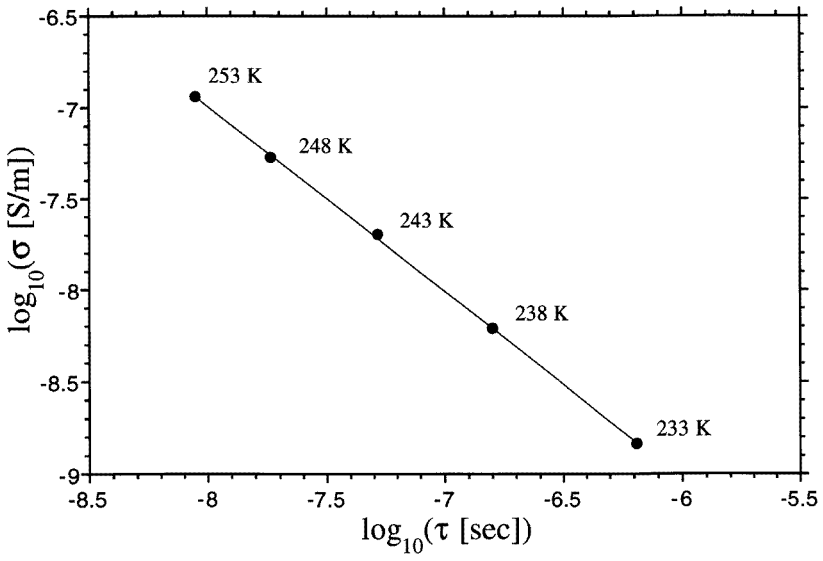

Figure 9. $\log_{10}(\sigma)$ versus $\log_{10}(\tau)$ for the temperatures indicated. The solid line represents the fitting equation $\sigma\tau^s$ = constant (where $s = 1.01 \pm 0.01$ and the constant $= (7.6 \pm 1.2) \times 10^{-16}$ F m^{-1}).

For our system, and for the temperatures indicated, the strongly coupled behaviour of the conductivity and relaxation time is evident in figure 9. The data reported on a log–log plot are well fitted by a straight line with slope -1; thus our system verifies equation (7*a*) well.

Very recently, Stickel *et al* [1, 2] showed, by a very accurate analysis, that the dynamics of the relaxation in many glass-forming liquids is well represented by a VF equation for temperatures above a certain temperature T_B, located some tenths of degrees above the glass transition temperature. The authors also found that between T_B and T_g the dynamics can be described either by another VF equation or by a different equation. This analysis requires very accurate data, spanning a wide temperature interval; it is based on the linearization of the VF equation and the consequent elimination of the pre-exponential factor. The elimination of this factor allows one to compare different observables chosen to characterize the dynamics of the system. On this basis, we analysed the data for both the conductivity and relaxation time for our compound using the same procedure as was employed by Stickel *et al* [1, 2].

The procedure that they proposed defines the new variables Φ and Θ [1]:

$$\Phi = \left[\frac{\mathrm{d}(\log_{10} x)}{\mathrm{d}T}\right]^{-1/2} = (B \log_{10} \mathrm{e})^{-1/2}(T - T_0) \tag{8}$$

$$\Theta = \frac{\mathrm{d}(\log_{10} x)}{\mathrm{d}T} \Big/ \frac{\mathrm{d}^2(\log_{10} x)}{\mathrm{d}T^2} = -\frac{1}{2}(T - T_0) \tag{9}$$

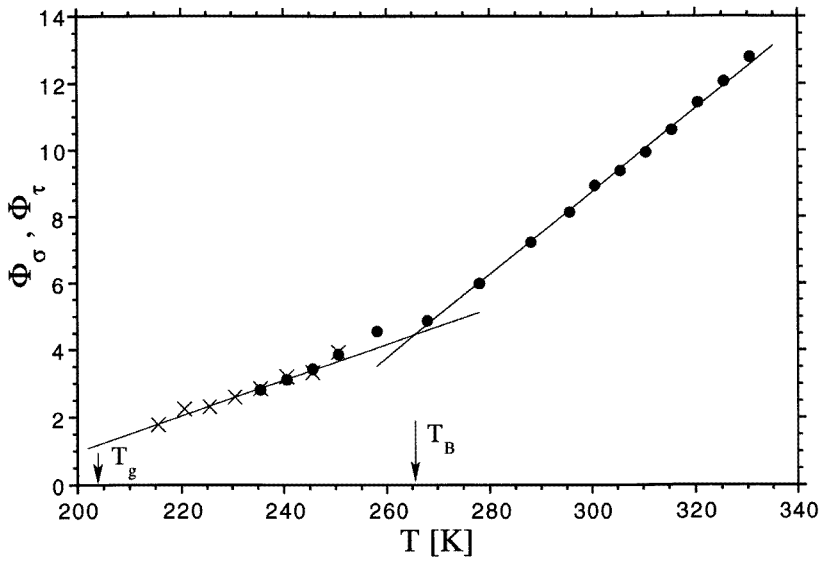

Figure 10. Φ as defined by equation (8) versus temperature. The data are from the d.c. conductivity σ (full points) and from the dielectric relaxation time τ (crosses). The solid lines which represent the fitting equations, describing the different VF behaviours in figure 8(b), cross at $T_B = 265$ K.

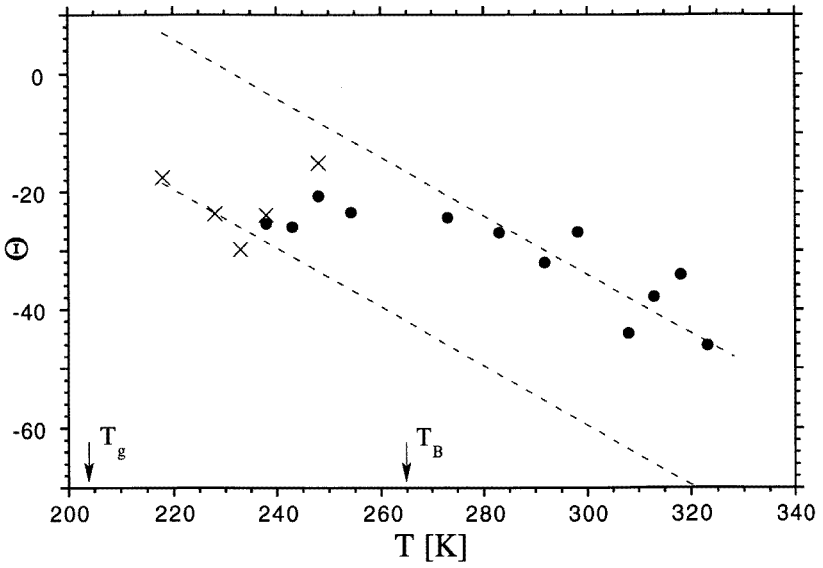

Figure 11. Θ as defined by equation (9) versus temperature. The data are from the d.c. conductivity σ (full points) and from the dielectric relaxation time τ (crosses). The dashed lines with slopes $-1/2$ correspond to the different VF behaviours in figures 8(b) and 10.

where x can be either σ or $1/\tau$, and the right-hand sides of equations (8) and (9) are calculated using the VF equation. The values of Φ versus temperature, numerically calculated from the data of figures 7 and 8(a) for τ and σ, respectively, are plotted in

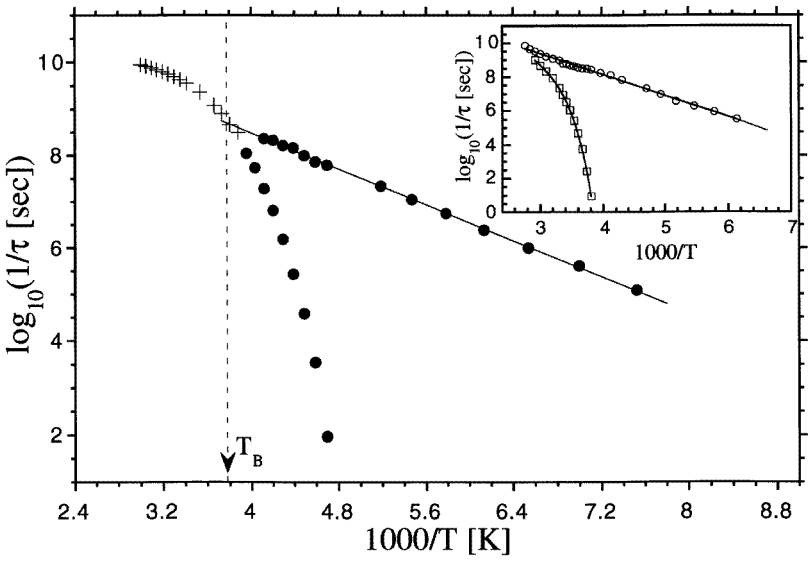

Figure 12. The relaxation times τ for the main and the secondary relaxations versus the reciprocal temperature $1/T$. The data are from the direct experimental values (full points) and from the conductivity (crosses). The fit of the secondary relaxation times (solid line) reaches the main relaxation times at just about T_B. The inset shows the relaxation times of DGEBA.

figure 10: they align on two straight lines which cross at the temperature $T_B \cong 265$ K. Though less accurate, even the values of the quantity Θ show that a transition between two regimes occurs (figure 11; the dashed lines represent again the two VF equations of figure 8(b)); this result is quite comparable to those discussed in the references previously quoted [1, 2]. It is reasonable to assume the validity of equation (7*a*) even outside the temperature interval of figure 9, especially at higher temperatures [2]. Accordingly, for temperatures above 253 K the time relaxation values can be calculated from the conductivity data using equation (7*a*); it is enough to extract from the fit of the data in figure 9 the constant value of the product $\sigma\tau$, for which the result is $(7.6 \pm 1.2) \times 10^{-16}$ F m^{-1}. A large error is apparent, which is however irrelevant for the following discussion concerning the relaxation time data. The calculated values of the relaxation times match well the trend of the direct experimental values (figure 12), and the secondary relaxation seems to merge into the main one at just about the transition temperature T_B. The coincidence of the transition temperature T_B, at which the main relaxation changes its behaviour, with the temperature of the splitting has been recently recognized for ortho-terphenyl and some other glass-forming liquids by Hansen *et al* [3]. Very precise dielectric measurements of the α-process of salol also revealed a crossover between two relaxation regimes at around 265 K [1], i.e. very close to the temperature where light-scattering investigations observed the development of a two-step relaxation process [34].

Though this behaviour, in our system, should be confirmed by direct measurements of the relaxation time (not at all easy), it is interesting to note that it differs from that observed for DGEBA (see the inset in figure 12) [25], where the main relaxation seemingly originates from the secondary one. The relaxation behaviour in the splitting region and its relationship with the microscopic structure are interesting points which need further experimental investigation and more accurate data [26]. This point will be considered

again in the following, when the data concerning the relaxation strengths are discussed. The observed influence of the onset of the secondary relaxation process on the main relaxation dynamics is reasonable, and should correspond to a progressive redistribution of the energy over the internal degrees of freedom either related to the particular molecular structure, i.e. segmental and side chain motions, or related to localized diffusive motions, i.e. Johari–Goldstein-like relaxations. In our opinion, from a general point of view, the unique relaxation observed for high temperatures above the splitting should be considered as distinct from the multiple relaxations which occur below the splitting temperature. In fact, as the temperature is raised above that of the glass transition, the multiple relaxations can merge by overlapping their relaxation time distributions; from this point on, the unique relaxation can eventually include all or some of the previous relaxations, which are no longer distinguishable. In this view, the merged relaxations can be more or less different from those relaxations which have collapsed together [26]. As a final remark, it has to be considered that under the conditions where equation (7*a*) applies, conductivity can provide reliable relaxation time data for exploring frequency regions that are not otherwise easily accessible.

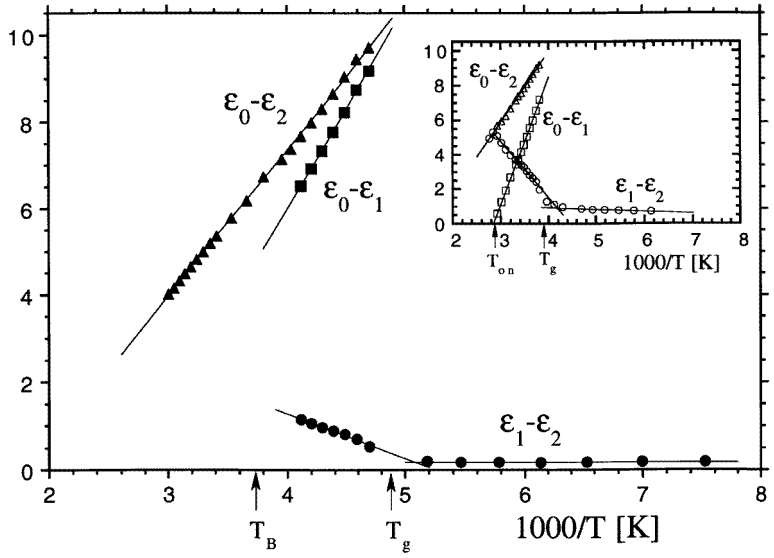

Figure 13. The overall relaxation strength (triangles), and the main (squares) and secondary (full points) relaxation strengths plotted versus the reciprocal temperature $1/T$ for CGE. The inset shows the same quantities for DGEBA.

3.4. Relaxation strengths

The analysis of the relaxation strengths represents a significant way of looking at the onset and at the change of the various relaxation modes occurring in a system when the temperature is varied [25]. In figure 13 we have plotted the overall relaxation strength, $\varepsilon_0 - \varepsilon_2$, the relaxation strength of the main process, $\varepsilon_0 - \varepsilon_1$, and the secondary relaxation strength, $\varepsilon_1 - \varepsilon_2$. The trends of these quantities versus reciprocal temperature can be considered almost linear; the slope of the secondary relaxation strength changes across the glass transition. A similar behaviour was observed for DGEBA [25], as is shown in the inset of figure 13. However,

the secondary relaxation of DGEBA does not seem to originate from the main relaxation; in fact, the former increases up to the value of the overall relaxation strength as the latter goes to zero at $T = T_{on}$. In the present system, the main relaxation strength depends linearly on the reciprocal temperature, and would vanish at a temperature situated well above the temperature T_B, where it is expected that the multiple relaxations overlap to give an overall relaxation strength only. On the basis of the experimental data, we are not able to explain what happens to the relaxation strengths for temperatures very close to and higher than T_B; this remains an open question, which merits further experimental investigation. Below the glass transition, the relaxation strength remains almost stable, although in other systems a slight increase with temperature is generally observed [20, 25, 35].

3.5. Shape parameters

The shape parameters, m and n, defined by the relations

$$m_1 = 1 - \alpha_1 \qquad n_1 = (1 - \alpha_1)\beta_1$$
$$m_2 = 1 - \alpha_2 \qquad n_2 = (1 - \alpha_2)\beta_2$$

represent the low- and the high-frequency tails of the two relaxations [36, 37]:

$$\varepsilon'' \propto \begin{cases} \omega^m & \text{for } \omega \ll \omega_0 \\ \omega^{-n} & \text{for } \omega \gg \omega_0 \end{cases}$$

where ω_0 is the angular frequency at the maximum of ε''.

As for DGEBA [25], the m- and n-parameters of CGE depend on temperature (figures 14(a) and 14(b)), so a time–temperature scaling law cannot be applied. The values of these parameters are predicted by a model which was specifically developed for amorphous polymers [38] on the following physical basis:

(i) the relaxation at frequencies much higher than the maximum dielectric loss frequency is related to local motions;

(ii) for frequencies much lower than the maximum dielectric loss frequency, the relaxation is dominated by large-scale motions.

According to this model, the values of the m- and n-parameters are positive and less than 1 and 0.5, respectively. Moreover, the increase of m and n with temperature is explained by a corresponding reduction of the intermolecular and intramolecular interactions.

The physical idea underlying this model can be exploited also to interpret the behaviour of simple glass-forming liquids, though, in this case, n can attain values higher than 0.5, as predicted for polymers [39].

By analysing our system under this scheme, we can give a rationale for the observed experimental behaviour of the m- and n-parameters. The stronger increase of m_1 and m_2 with temperature with respect to that of the ns could indicate that the intermolecular interactions are much more affected by the temperature. The corresponding small increase of the n-parameters can probably be ascribed to a limited increase of the mobility of the internal parts of the molecules. In particular, the parameter m_2 of the secondary relaxation (figure 14(b)) shows a marked change of the slope going through the glass transition temperature. This result demonstrates that not only the strength, but also the shape of the secondary relaxation is modified by the glass transition. The analysis performed on the CGE system closely parallels the one that was performed on DGEBA [25]; the two systems provide quite comparable results, which agree well with theoretical predictions.

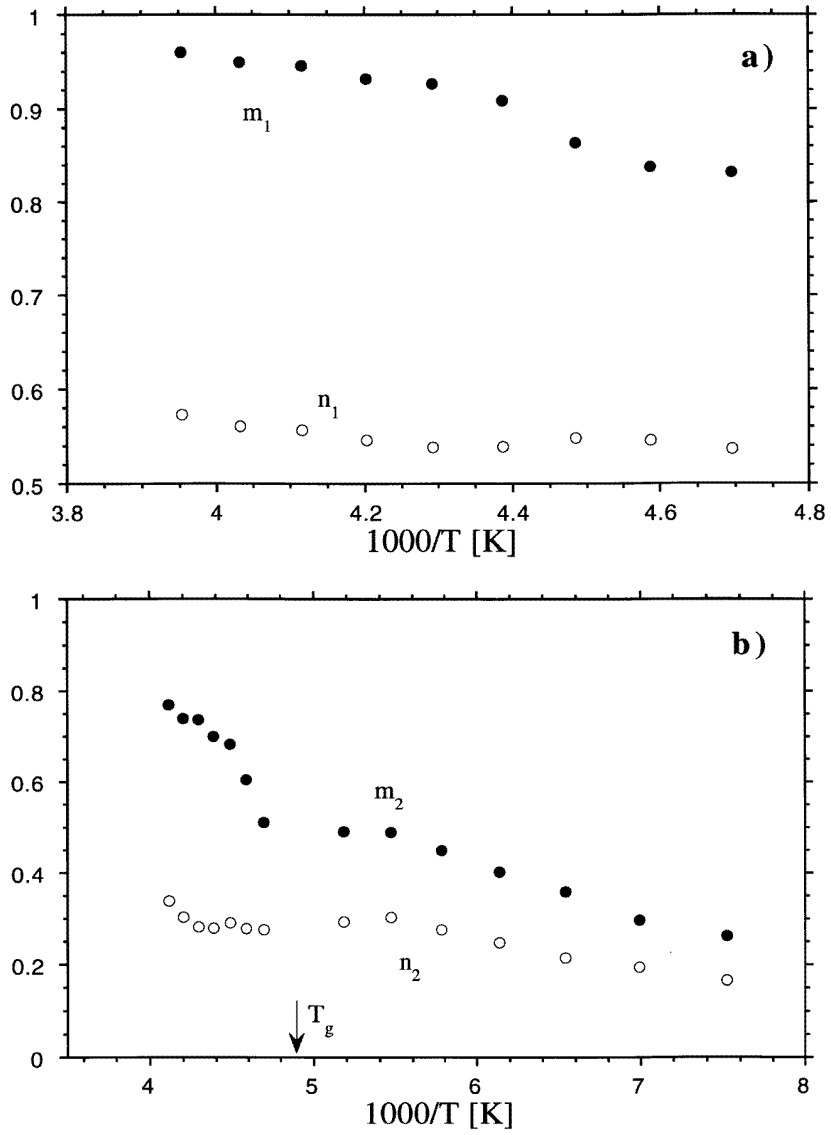

Figure 14. The shape parameters m and n of (a) the main and (b) the secondary relaxation plotted versus the reciprocal temperature $1/T$ for CGE.

4. Conclusions

The data analysis presented here has indicated that all of the dielectric parameters, either directly measured or extracted by means of a fitting procedure, provide significant information on relaxation processes. The conductivity data confirmed the existence of a temperature, T_B, at which a transition occurs between two relaxation regimes, each described by a different VF equation, as previously observed in references [1–3]. The relaxation times describe accurately the dynamics of the systems by providing a value for the glass transition temperature, and giving information on the splitting between the main

and secondary relaxation processes. In the high-temperature region the two observables, the conductivity and main relaxation time, can be related to each other, so the highest relaxation times, not easy to measure directly, were calculated from the conductivity data. The Arrhenius plot of the relaxation times indicated that the splitting region occurs at around the temperature T_B. We believe that the relaxation at high temperature should be in principle considered different from both the main and secondary relaxations that we observe below the splitting temperature.

The behaviour of CGE parallels that of DGEBA: in particular, at the glass transition a change in the slope of the secondary relaxation strength was observed, and the shape parameter values were found to agree with the theoretical predictions. Concerning the relaxation strengths, the behaviour of CGE is only partly similar to that of DGEBA; however, the different splitting layout and the lower value of the splitting temperature suggest that one should avoid any interpretation which could place too much emphasis on the present experimental results.

References

[1] Stickel F, Fischer E W and Richert R 1995 *J. Chem. Phys.* **102** 6251
[2] Stickel F, Fischer E W and Richert R 1996 *J. Chem. Phys.* **104** 2043
[3] Hansen C, Stickel F, Berger T, Richert R and Fischer E W 1997 *J. Chem. Phys.* submitted
[4] McCrum N G, Read B E and Williams G 1967 *Anelastic and Dielectric Effects in Polymeric Solids* (New York: Dover)
[5] Jäckle J 1986 *Rep. Prog. Phys.* **49** 171
[6] Giordano M, Leporini D and Tosi M P (ed) 1996 *Proc. Non-equilibrium Phenomena in Supercooled Fluids, Glasses and Amorphous Materials* (Singapore: World Scientific)
[7] Johari G P and Goldstein M 1970 *J. Phys. Chem.* **74** 2034
[8] Johari G P and Goldstein M 1970 *J. Chem. Phys.* **53** 2372
[9] Johari G P and Goldstein M 1971 *J. Chem. Phys.* **55** 4245
[10] Johari G P and Smyth C P 1972 *J. Chem. Phys.* **56** 4411
[11] Johari G P 1973 *J. Chem. Phys.* **58** 1766
[12] Pochan J M, Gruber R J and Pochan D F 1981 *J. Polym. Sci., Polym. Phys. Edn* **19** 143
[13] Ochi M, Shimbo M, Saga M and Takashima N 1986 *J. Polym. Sci.* B **24** 2185
[14] Ochi M, Yoshizumi M and Shimbo M 1987 *J. Polym. Sci.* B **25** 1817
[15] Sheppard N F Jr and Senturia S D 1989 *J. Polym. Sci.* B **27** 753
[16] Gangasharan and Murthy S S N 1993 *J. Chem. Phys.* **99** 9865
[17] Hofmann A, Alegría A, Colmenero J, Willner L, Buscaglia E and Hadjichristidis N 1996 *Macromolecules* **29** 129
[18] Garwe F, Schönhals A, Beiner M, Schröter K and Donth E 1994 *J. Phys.: Condens. Matter* **6** 6941
[19] Fioretto D, Livi A, Rolla P A, Socino G and Verdini L 1994 *J. Phys.: Condens. Matter* **6** 5295
[20] Arbe A, Richter D, Colmenero J and Farago B 1996 *Phys. Rev.* E **54** 3853
[21] Floudas G F, Higgins J S, Kremer F and Fischer E W 1992 *Macromolecules* **25** 4955
[22] Shi J-F, Inglefield P T, Jones A A and Meadows M D 1996 *Macromolecules* **29** 605
[23] Garwe F, Beiner M, Hempel E, Schawe J, Schröter K, Schönhals A and Donth E 1994 *J. Non-Cryst. Solids* **172–174** 191
[24] Reinhardt M, Schönhals A, Pfeiffer D, Pfeiffer K, Lampe I V and Lorkowski H J 1996 *Polym. Adv. Technol.* **7** 791
[25] Casalini R, Fioretto D, Livi A, Lucchesi M and Rolla P A 1997 *Phys. Rev.* B submitted
[26] Garwe F, Schönhals A, Lockwenz H, Beiner M, Schröter K and Donth E 1996 *Macromolecules* **29** 247
[27] Butta E, Livi A, Levita G and Rolla P A 1995 *J. Polym. Sci.* B **33** 2253
[28] Havriliak S and Negami S 1986 *J. Polym. Sci., Polym. Symp.* **14** 89
[29] Vogel H 1921 *Phys. Z.* **22** 645
[30] Tammann G and Hesse W 1926 *Z. Anorg. Allg. Chem.* **156** 245
[31] Koike T and Tanaka R 1991 *J. Appl. Polym. Sci.* **42** 1333
[32] Koike T and Tanaka R 1993 *Polym. Eng. Sci.* **33** 1301
[33] Deng J and Martin G C 1994 *Macromolecules* **27** 5141

[34] Li G, Du W M, Sakai A and Cummins H Z 1992 *Phys. Rev.* A **46** 3343
[35] Smith G D and Boyd R H 1991 *Macromolecules* **24** 2731
[36] Casalini R, Livi A, Rolla P A, Levita G and Fioretto D 1996 *Phys. Rev.* B **53** 564
[37] Jonscher A K 1996 *Universal Relaxation Law* (London: Chelsea Dielectric)
[38] Schönhals A and Schlosser E 1989 *Colloid Polym. Sci.* **267** 125
[39] Schönhals A, Kremer F and Schlosser E 1991 *Phys. Rev. Lett.* **67** 999